Distribution of DNA damage in the sperm nucleus: A study of zebrafish as a model of histone-packaged chromatin

S. González-Rojo[a], C. Fernández-Díez[a], M. Lombó[a], M.P. Herráez[a], *

[a] *Department of Molecular Biology, Faculty of Biology, Universidad de León, Campus de Vegazana s/n León, 24071, Spain*

A B S T R A C T

Reproductive defects can occur when the integrity of the male gamete genome is affected. Sperm chromatin is not homogeneous, having relaxed regions which are more accessible to the transcription machinery in the embryo, and thought to be specially sensitive to DNA damage. The level of damage in specific genes located in these sensitive regions could represent an early biomarker of damage. Our objective is to test the hypothesis that these more relaxed regions show greater susceptibility to damage in zebrafish, a species lacking protamines and whose sperm chromatin is compacted with histones. After sperm UV irradiation, treatment with H_2O_2 and cryopreservation, global chromatin fragmentation was evaluated using the TUNEL assay, and the number of lesions per 10 Kb in specific genes (*hoxa3a, hoxb5b, sox2,* accessible for early transcription and *rDNA 18S* and *rDNA 28S*) was quantified by using a qPCR approach. Additionally, oxidative damage within the sperm nucleus and the potential colocalization of this injury with histone H3 and TOPO IIα+β were located by using immunofluorescence. UV irradiation produced the highest degree of fragmentation ($p = 0.041$) and the highest number of lesions per 10 Kb in all the genes, but no differences were observed in sensitivity to damage in the studied genes (ranging from 14.93 to 8.03 lesions per 10 Kb in *hoxb5b* and *28S,* respectively). In contrast, H_2O_2 and cryopreservation caused varying levels of damage in the analyzed genes which was not related to their accessibility, ranging from 0.00 to 1.65 lesions per 10 Kb in *28S* and *hoxb5b*, respectively, after H_2O_2 treatment, and from 0.073 to 5.51 in *28S* and *sox2*, respectively, after cryopreservation. Immunodetection near oxidative lesions also revealed different spatial patterns depending on the treatments used, these being mostly homogeneous with UV irradiation or cryopreservation, and peripherally located around the nucleus after H_2O_2 treatment. Oxidative lesions did not colocalize with histone H3 or TOPO IIα+β, thus demonstrating that the relaxed DNA regions associated with these proteins were not more vulnerable to oxidative damage. Results suggest that accessibility of each agent to the nucleus could be the main factor responsible for the distribution of sperm DNA damage rather than the organization of the chromatin. Lesions in these genes important to early embryo development assayed in this study cannot be used as biomarkers of global DNA damage.

© 2018.

1. Introduction

Detection of DNA damage in the male germ line is a key point in sperm quality evaluation, and has gained importance since Evenson and colleagues established a relationship between chromatin structure and seminal fertility [1]. Sperm chromatin is not simply an "inert" chromatin; the role of specific paternal genes from their initial development is now accepted as crucial [2].

Sperm chromatin has a unique architecture, determined by DNA and associated sperm nuclear basic proteins (SNBPs), which package chromatin during spermatogenesis, when histones are replaced by protamines. However, this process varies throughout the Animal kingdom. Mammalian sperm DNA is packed by protamines into toroids, a configuration believed to hinder access by damaging agents (such as reactive oxygen species, ROS) to the DNA strand, thus pro-

viding sperm with protection against injuries. A small fraction of chromatin remains wrapped in histones, forming nucleosomes, and a DNA fraction is attached to the sperm nuclear matrix between each toroid [3–5]. The retained nucleosomal fraction has been described as the region harboring loci of developmental importance [4,6] and postulated as more susceptible to DNA damage. The regions attached to the nuclear matrix are also vulnerable due to their relaxed inner conformation [7,8]. The existence of particular DNA areas more susceptible to harmful agents could help to identify specific genes, located in these regions, as biomarkers of DNA damage, providing refined targets to evaluate the genomic conformity of a given seminal sample. To confirm this hypothesis, it is necessary to analyze distribution of damage caused by different genotoxic treatments. Greater susceptibility of the nucleosomal regions to DNA oxidation was observed by Noblanc and colleagues [9] in epididymal sperm of mice defective in antioxidant systems. However, after ejaculation different agents can increase oxidative stress and promote DNA damage, the distribution of which could be determined by additional factors unrelated to the chromatin structure.

* Corresponding author.
Email address: paz.herraez@unileon.es (M.P. Herráez)

Fish represent a different scenario because sperm chromatin condensation by SNBPs is highly variable; some species such as rainbow trout (*Oncorhynchus mykiss*) totally replace histones by protamines, whereas others maintain somatic-like histones, with no traces of protamines, as is the case of zebrafish (*Danio rerio*) [10–12]. Using different injuring treatments, our group demonstrated in rainbow trout sperm, lacking histones, that DNA damage distribution was not related to the presence of SNBPs, which suggests that factors other than SNBPs permit damaging agents to access the DNA helix [11]. Zebrafish sperm is packaged by histones, with higher level of linker histone H1 than a somatic cell [12]. In spite of harboring only histones, therefore, zebrafish sperm chromatin exhibits differential packaging, which is also represented by the distribution of epigenetic marks (covalent modifications of DNA and associated histones that do not affect the genetic code). Specific blocks of chromatin, with a low DNA methylation status and particular histone modifications, harbor early transcribed genes required for embryo development, with similar features to those recognized in histone-bound regions in mammals [12].

In this study, we aim to evaluate differential susceptibility to genotoxic damage in the nucleus of zebrafish spermatozoa and to test the hypothesis that nucleosomal regions or early transcribed genes show greater sensitivity to DNA damage. To underline the potential importance of chromatin structure/accessibility in the distribution of damage, different treatments -which differentially affect DNA, promoting diverse kinds of lesions and showing differential genotoxic potential-were applied: irradiation with UV, treatment with a potent oxidizer (H_2O_2), and cryopreservation. Analysis of (i) global fragmentation, (ii) number of lesions in genes located in different chromatin regions, and (iii) specific localization of oxidative damage, will enable us to determine whether chromatin structure is a primary factor involved in susceptibility to damage.

2. Materials and methods

2.1. Reagents

Unless otherwise indicated, all components used were purchased from Sigma (Sigma Aldrich Spain, Madrid).

2.2. Animal maintenance

Zebrafish (*Danio rerio*) were manipulated in accordance with the Guidelines of the European Union Council (2010/63/EU), following Spanish regulations (RD 1201/2005, abrogated by RD 53/2013) and specifically approved by the Research Ethical Committee of the University of León. Six-month-old wildtype zebrafish (AB strain) were maintained in 2.5 L aquaria (ZebTEC, Tecniplast System, Italy) in a recirculating water system (pH 7.0–7.5, 450–500 μS at 27–29 °C, 14:10 light-dark cycle). The animals were fed twice a day with dry food (Special Diets Services®, UK) and live brine shrimps.

2.3. Gamete collection

The zebrafish were anesthetized with 168 mg/L of ethyl 3-aminobenzoate methanesulfonate (MS-222). Sperm was extracted by ventral squeezing (procedure by Carmichael and colleagues [13]). Samples from ten males were pooled and diluted in 20 μL of Hank's Solution (137.0 mM NaCl, 5.32 mM KCl, 0.25 mM Na_2HPO_4, 0.44 mM KH_2PO_4, 1.29 mM $CaCl_2$, 1.0 mM $MgSO_4$ and 4.17 mM $NaHCO_3$; 280 mOsm/kg) at 4 °C.

Only those samples which met the standards for volume and cell count were selected (0.5 μL and $1 \cdot 10^7$ cells/mL, respectively). Three pools of zebrafish sperm (ten males per pool) were studied.

2.4. Exposure to damaging agents

Each sperm pool was split into four aliquots to be subjected to different treatments: UV irradiation (254 nm, 400 μW/cm^2 – Vilber (Germany) –, 10 min at 15 cm from the lamp), hydrogen peroxide (freshly prepared 250 mM, 20 min) and cryopreservation. Non-treated samples were used as controls. Treatments were carried out in a final volume of 100 μL (approximately 1–4·10^7 cells/mL) at 4 °C. Cryopreservation was performed following the indications by Carmichael and colleagues [13]. Briefly, the sperm samples were cryopreserved by diluting the milt pool in 20 μL of extender solution (absolute methanol diluted 1/10 (v/v) in Ginsburg Fish Ringer's solution – 111.23 mM NaCl, 3.35 mM KCl, 2.70 mM $CaCl_2$, 2.38 mM $NaHCO_3$ – with 0.15 g/mL added skim milk). Ten μL of this mix was placed in a 2 mL cryovial which was then placed in a 15 mL tube, and immersed in dry ice for 20 min before being stored in liquid nitrogen. The sperm samples were thawed at 33 °C for 8–10 s. After each treatment, they were centrifuged at 2000g for 5 min and washed with Hank's solution. Oxidative stressed and cryopreserved milt samples were additionally washed with Hank's solution to remove H_2O_2 or cryoprotectant remains.

2.5. TUNEL assay

DNA fragmentation was assessed using a commercial kit (In Situ Cell Death Detection Kit, Fluorescein, Roche, Germany) following the manufacturer's instructions with slight modifications: permeabilization of sperm cells was carried out with 0.3% Triton X-100 in 0.1% sodium citrate for 5 min, and the DNaseI concentration used for the treatment of positive controls was 70 U/mL. Nuclei were counterstained with 300 nM DAPI for cell visualization. For each milt pool (n=3), two slides were evaluated using a Nikon Eclipse TE-2000 EZ.C1 confocal microscope equipped with a 408 nm and 488 nm excitation source for DAPI and FITC staining. Negative (without terminal transferase) and positive controls were included and the assay was carried out in duplicate. Approximately 200 cells were analyzed per slide using ImageJ software. The results were expressed as the percentage of cells with fragmented DNA (mean ± SD).

2.6. Quantification of DNA lesions in genes

2.6.1. Genomic DNA isolation

The pellets obtained after treatments were resuspended in a final volume of 500 μL TNES buffer (10 mM Tris-HCl pH 8.0, 125 mM NaCl, 10 mM ethylenediaminetetraacetic acid (EDTA), 17 mM sodium dodecyl sulfate (SDS), 4 M urea) with 1 μg proteinase K and incubated overnight at 56 °C in a shaking bath. After proteinase K digestion, DNA was extracted using an optimized phenol:chloroform method [11].

DNA quantity and quality were determined using Nanodrop 1000 (Thermo Scientific) at 260 nm. Only high purity DNA ($A_{260}/A_{280} > 1.8$) was used for the subsequent analysis.

2.6.2. Quantitative PCR

The number of lesions in DNA was determined using the method developed by Rothfuss and colleagues [14]. Real time PCR was performed in triplicate on a Step-One Plus real-time thermal cycler (Applied Biosystems) and non-template control was used for each pair of

primers. Design of oligonucleotides was carried out with Primer Express 2.0 software. Amplification efficiency was determined for all nucleotides using serial dilutions of gDNA and calculated with StepOnePlus version 2.3 software using the linear regression slope of the dilution series (Table 1). Reaction conditions were as described elsewhere [11] and required 3 ng of gDNA. Reaction conditions were a pre-incubation phase of 10 min at 95 °C, followed by 50 cycles of 10 s at 95 °C, 10 s at the annealing temperature (see Table 1) and 50 s or 10 s (for long and short amplicons, respectively) at 72 °C. Product specificity was verified by agarose gel electrophoresis (data not shown) and by melting curves and threshold cycles (C_ts) which were measured by StepOnePlus version 2.3 software. The number of lesions was studied in five nuclear genes (*hoxa3a, hoxb5b, sox2, rRNA 18S and rRNA 28S*).

The number of DNA lesions per 10 Kb with respect to the basal level of lesions in non-treated samples was analyzed in each pool independently and calculated according to formula [14]:

$$Lesion\ rate = 1 - 2^{-(\Delta Ct\ long\ -\ \Delta Ct\ short)} \times \frac{10000\ (bp)}{size\ of\ long\ fragment\ (bp)}$$

Mean ± SD were calculated.

2.7. Immunolocalization of 8-OHdG

Samples were fixed with 4% (w/v) paraformaldehyde in PBS (8.37 mM Na_2HPO_4, 1.83 mM KH_2PO_4, 149.9 mM NaCl, pH 7.4; 335 mOsm/kg) for 20 min at room temperature, washed three times with bi-distilled water and diluted to a final concentration of $5·10^6$ cells/mL. For each sperm pool (n=3), twenty μL was smeared on ATE ([3-aminopropyl]trimethoxysilane) coated slides in triplicate and left to desiccate at 37 °C overnight. Following the method of González-Rojo and colleagues [11], we incubated with the primary antibody against 8-OHdG (ab62623, "anti-DNA/RNA damage antibody", Abcam, Cambridge, UK) (dilution 1/200) overnight at 4 °C. Incubation with a goat anti-mouse secondary antibody labelled with orange-red AlexaFluor®568 (Invitrogen, Camarillo, CA, USA) was at 37 °C for 1 h. Negative controls with normal goat serum were included. Nuclei were stained with 300 nM DAPI and slides were mounted using ProLong® Gold Antifade Mountant (Thermo Scientific). Images were captured with a Nikon Eclipse TE-2000 confocal microscope.

2.8. Colocalization of 8-OHdG with histone H3, TOPO IIα+β

Double immunofluorescence on non-treated and H_2O_2 treated samples was performed following the protocol described above, with modifications to the primary antibody incubation. Primary antibody dilutions were: 1/200 mouse monoclonal 8-OHdG antibody (ab62623, "anti-DNA/RNA damage antibody", Abcam, Cambridge, UK); 1/20 rabbit monoclonal TOPO IIα+β antibody (ab109524, Abcam, Cambridge, UK) and 1/200 rabbit polyclonal Histone H3 antibody (ab1791, Abcam, Cambridge, UK). Each specific antigen was revealed with a solution containing two secondary antibodies: goat anti-rabbit IgG (H + L) AlexaFluor®488 and goat anti-mouse IgG (H + L) AlexaFluor®568 (Invitrogen, Camarillo, CA, USA). Negative controls were included as described above. Images were captured with a confocal microscope Zeiss LSM800 and merged images were created with ZEN Blue software (Zeiss).
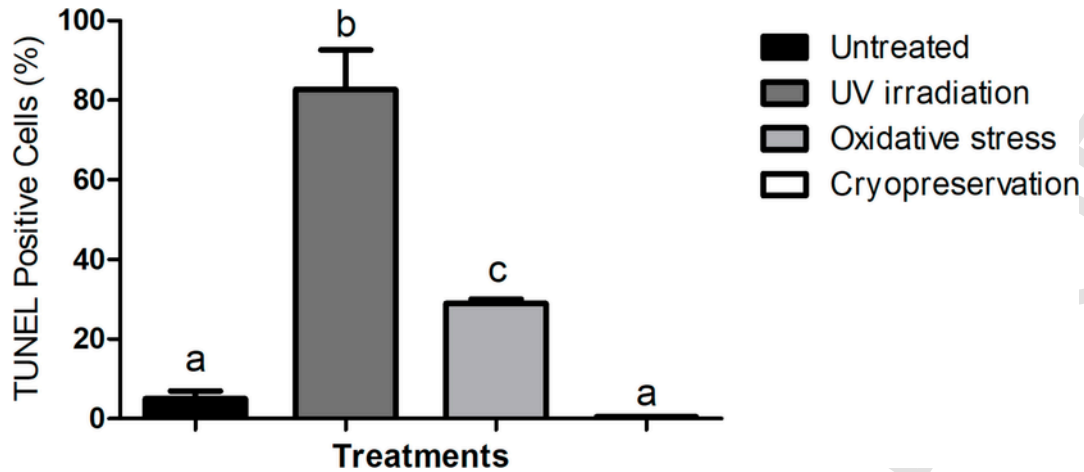
2.9. Statistical analysis

Statistical analysis was performed with SPSS version 21.0 (IBM, EEUU). Normality of data was checked by the Shapiro-Wilk test. Due to the non-parametric nature of the data, a Kruskal-Wallis test was performed using Dunn's post hoc test ($p < 0.05$). The results are shown as mean ± SD.

3. Results

The TUNEL assay showed that control samples exhibited a basal level of DNA fragmentation (less than 5% positive cells) in all the analyzed pools. UV irradiation showed the highest rate of DNA fragmentation, affecting 82.72% ± 8.11 ($p = 0.041$, with respect to the untreated samples) of zebrafish spermatozoa (Fig. 1). Oxidative stress promoted by H_2O_2 also produced an increase in DNA fragmentation (28.98% ± 0.88; $p = 0.041$, with respect to non-treated sperm, Fig. 1); whereas cryopreservation did not alter sperm chromatin integrity when compared to the untreated sperm.

No significant differences in the number of lesions, in relation to the basal level of lesions in non-treated samples, were observed among genes after UV or oxidative stress treatments (Fig. 2). UV promoted from 14.93 ± 0.26 to 8.03 ± 5.57 lesions per 10 Kb in *hoxb5b* and *28S*, respectively. Oxidative stress caused the highest level of damage in *hoxb5b* (1.65 lesions per 10 Kb ± 1.23). Lesions after cryopreservation showed different sensitivity among genes, ranging from 0.07 ± 0.10 in *28S* to 5.51 ± 0.63 in *sox2*.

Table 1
List of forward and reverse primers used in conventional PCR and qPCR assays for zebrafish samples. For all genes, their corresponding GenBank accession number is indicated, as well as the size of the amplicon, oligonucleotide efficiency and the annealing temperature. All sequences are given in the 5' direction.

Genes and GeneID	Forward oligonucleotide	Reversed oligonucleotide	PCR product size (bp)	PCR efficiency (%)	Annealing temperature (ºC)
hoxa3a	AGGATGTGCAGTGAGAACCAT	CCCACCAAAGAATCCGAGTA	669	95.2	58
58049	TGCTTAACCTGACGGAAAGG	TGTACTTCATCCTGCGATTC	60	92.2	58
hoxb5b	TTTCCAAAATCCGAGTCAGG	AATAATTTACCATGCAGTCGCC	649	92.8	58
58052	AGACCCGGTACAGACAGTCG	GGTGGCACAAGACAGAGGAT	62	100.7	58
sox2	ACGACGATTAACGGCACGAT	AAAAGCTGGAGAGTGCCTCTGT	650	94.0	55
Riesco MF 2013	TGCACAACTGATGTTTACGTCAAA	ATGTACCTTCAGTGAGAAACTCTTTAAATC	81	108.1	58
rRNA 18S	CAAGAACGAAAGTCGGAGGT	CCTCGTTGATGGGAAACAGT	612	102.9	55
FJ915075.1	GCCGTTCTTAGTTGGTGGAG	CCGGAGTCTCGTTCGTTATC	60	124.7	58
rRNA 28S	GCTCATCAGACCCCAGAAA	CCTGCCCTTCACAAAGAAA	578	106.6	55
AF398343.1	GAAGGCCGAAGTGGAGAAG	CCCTTAGGACCGACTGACC	66	92.3	58

Fig. 1. Chromatin fragmentation evaluated by the TUNEL assay. DNA damage is expressed as the percentage of FITC positive cells. Data are expressed as mean±SD and letters show differences among treatments (n=3, at least 200 cells analyzed per replicate, $p < 0.05$).
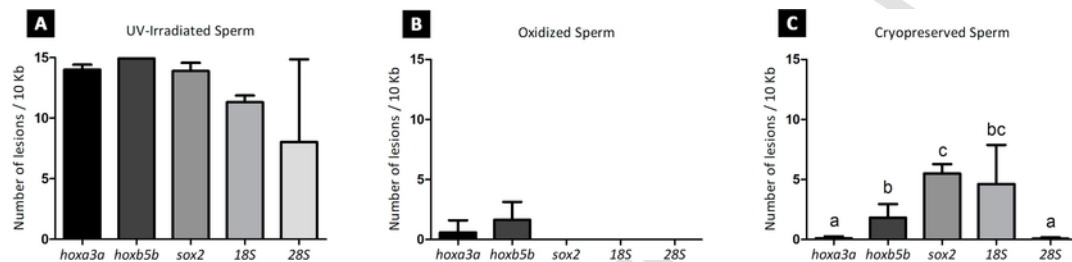
Fig. 2. Number of lesions per 10 Kb in specific genes after zebrafish sperm treatments. UV irradiation $400 \mu W/cm^2$ for 10 min (A), 250 mM H_2O_2 exposure for 20 min (B) and cryopreservation (C) induce different levels of damage. DNA damage was calculated as the DNA lesion rate respect to the basal level of lesions in non-treated samples. Data are expressed as mean±SD and letters show differences among genes for the same treatment (n=3 pools, $p < 0.05$).

In irradiated sperm, 8-OHdG was localized throughout the entire nucleus with some more intense spots in those cells presenting oxidation (Fig. 3B), clearly different from the untreated ones (Fig. 3A). After H_2O_2 treatment, 8-OHdG appeared in the nuclear periphery of the spermatozoa (Fig. 3C). After cryopreservation, a reduced number of cells displayed 8-OHdG homogeneously distributed around the nucleus (Fig. 3D).

Histone H3 is distributed throughout the nucleus, with more intensity in the nuclear periphery (Fig. 4). TOPO IIα+β is confined to a small specific region, displaying a clear and intense green spot (Fig. 4). As can be observed in Fig. 3B and D, oxidative lesions promoted by UV or cryopreservation, do not colocalize with any of these proteins (comparing Fig. 3B, D with Fig. 4). In H_2O_2-treated samples, 8-OHdG is restricted to the periphery, but not all the regions harboring H3 or TOPO IIα+β are affected by oxidation (Fig. 4, arrow heads).

4. Discussion

Distribution of DNA damage in the sperm nucleus is of utmost importance considering the differential role that paternal genes play during development. The elucidation of chromatin packaging has revealed different regions of DNA with a lower degree of compaction, which have been hypothesized as being more sensitive to DNA damage [7,8]. Fish display a more diversified pattern of chromatin condensation, some species presenting only one type of SNBPs, and as such could serve as a model to test this hypothesis. Previous results obtained by our group using rainbow trout (*Oncorhynchus mykiss*) sperm, whose chromatin is homogeneously compacted with protamines, show that localization of DNA damage is not dependent on the type of SNBPs, but rather it is the nature of the harmful treatment which is decisive [11].

The present study, which uses a model with a different chromatin packaging pattern, lacking protamines, permits evaluation and localization of DNA damage in the sperm nucleus subjected to different injuries. Zebrafish sperm chromatin is compacted with histones, with highly compacted regions or chromatosomes due to the presence of linker histone H1. Specific chromatin blocks, where genes with embryo development features are found [12], are modelled by epigenetic modifications, such as DNA hypomethylation, which define more accessible regions where early transcribed genes are located [6,12].

Sperm DNA damage can appear in the form of abasic sites, nucleotide base modifications, strand breaks or bond generation between DNA-binding proteins, among others. DNA alterations in the whole genome can be assayed with different methodologies such as the TUNEL assay, used in this study, which informs about DNA fragmentation. Our data obtained from TUNEL confirm the good quality of the untreated milt pools and show that the treatments used have different genotoxic potential, UV irradiation being the one which caused the highest level of fragmentation. However, to assess damage in specific genes, a different approach, based on qPCR technology, has been developed [14]. Quantification of DNA lesions using qPCR is based on the delay of DNA polymerase when alterations in DNA strand are found, whatever the type of lesion. This method provides measurements relating to the corresponding untreated sample, thus permitting quantification of the number of lesions in individual genes [14].

UV irradiation affects chromatin by generating ROS that produce base modifications, mainly oxidization, resulting in the production of
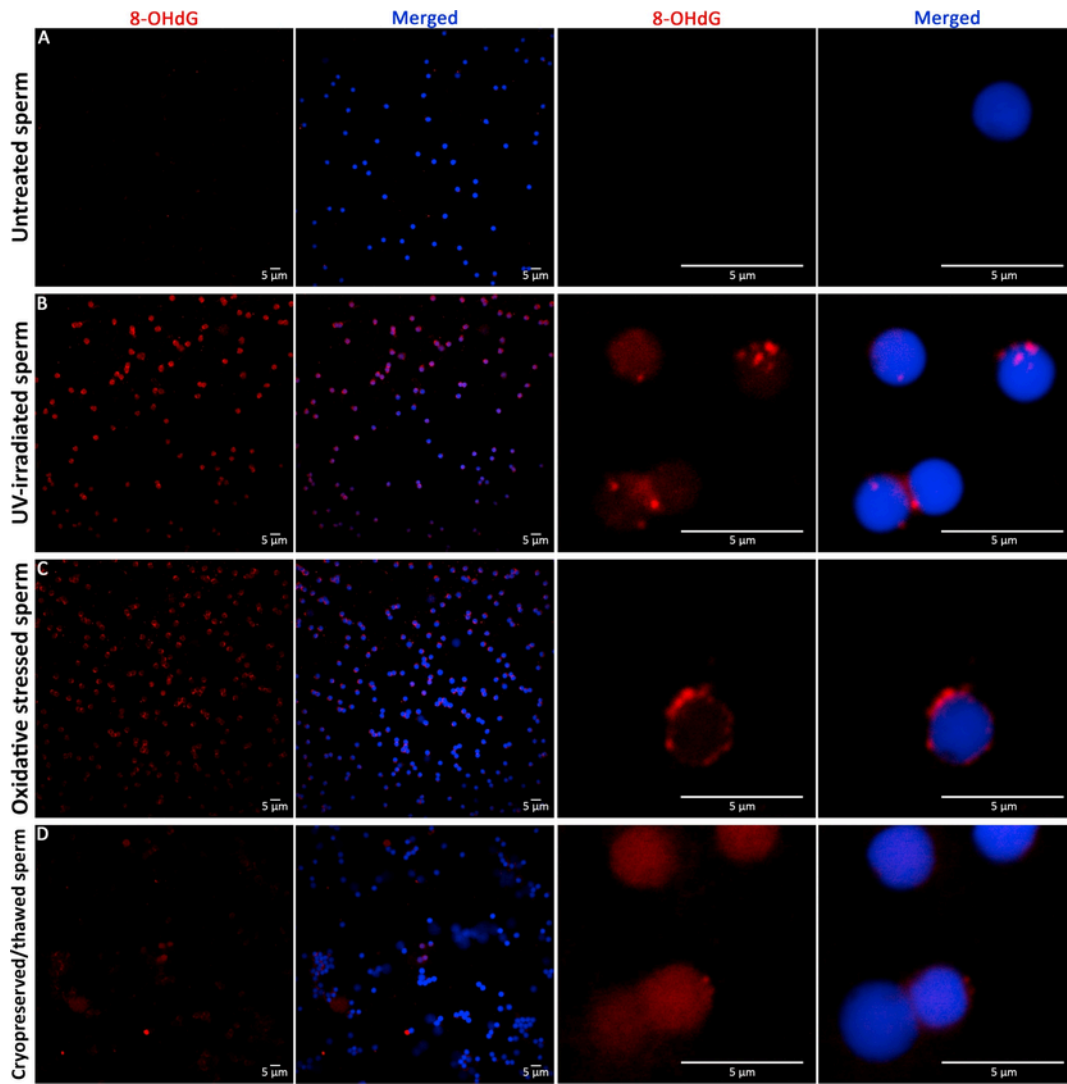
Fig. 3. Immunolocalization of oxidative damage within the sperm nucleus. Images show an example of zebrafish sperm cells in non-treated samples (A), in UV-irradiated milt (B), after H_2O_2 treatment (C) or frozen/thawed sperm (D). Sperm spreads ($5 \cdot 10^5$ cells/mL) were stained with an antibody recognizing 8-OHdG and its location appears in red fluorescence (AlexaFluor®568), whereas cell nuclei were stained with DAPI and appear in blue. Merged images were stacked using Image J software. Scale bar, 5 µm.

8-OHdG [15,16]. It also promotes the formation of cyclobutane pyrimidine dimers and chromatin fragmentation. In the present work, UV radiation promotes the greatest number of lesions in comparison to the rest of the treatments, as shown by the TUNEL and qPCR approaches. However, no differences among genes were noticed after UV treatment, regardless of the specific epigenetic pattern and the different degree of chromatin accessibility of each studied gene. In zebrafish sperm, *hoxa3a* and *hoxb5b* are among the 250 DNA hypomethylated genes and, together with the *sox2* gene, they possess specific histone modifications, which are characteristic of chromatin blocks harboring developmental genes [12] and of the most relaxed chromatin regions. The *18S* and *28S* rDNA genes do not share any of these characteristics [12], since they have a lower degree of accessibility. Global DNA damage has been reported after UV irradiation in other fish species such as rainbow trout sperm; in this species, the Comet assay, used to analyze single and double DNA strand breaks, revealed approximately 70% of cells with fragmented DNA after UV irradiation [17]. Hydrogen peroxide treatment, usually used to promote oxidative damage, caused DNA fragmentation at the tested dose and a significantly lower number of lesions than UV irradiation in the analyzed genes, without noticeable differences among them. In other species such as seabream (*Sparus aurata*) sperm, whose chromatin is homogeneously compacted by histones [18], our group also reported DNA fragmentation and lesions in two nuclear genes after treatment with a lower dose of H_2O_2 [19]. Cryopreservation affects DNA by ROS generation [20,21] or osmotic shock [22,23], causing fragmentation [24] and base oxidization [22]; however, in the present study cryopreservation did not promote a level of fragmentation detectable by TUNEL. Similar results were obtained after seabream sperm cryopreservation, where a minimum level of DNA fragmentation was revealed using the Comet assay [19]. In other species, such as rainbow trout, seabass (*Dicentrarchus labrax*) or salmon (*Salmo salar*), sperm DNA fragmentation was reported after cryopreservation using the Comet assay [25–28]. Freezing/thawing generated a different degree of lesions in genes analyzed by qPCR, *sox2* and *18S* having a similar number of lesions (around 5 lesions per 10 kb) in spite of their varying accessibility in sperm chromatin. These results imply that the analyzed genes have different susceptibility to DNA damage depending on the applied treatments, but not on specific chromatin organization or epigenetic pattern.
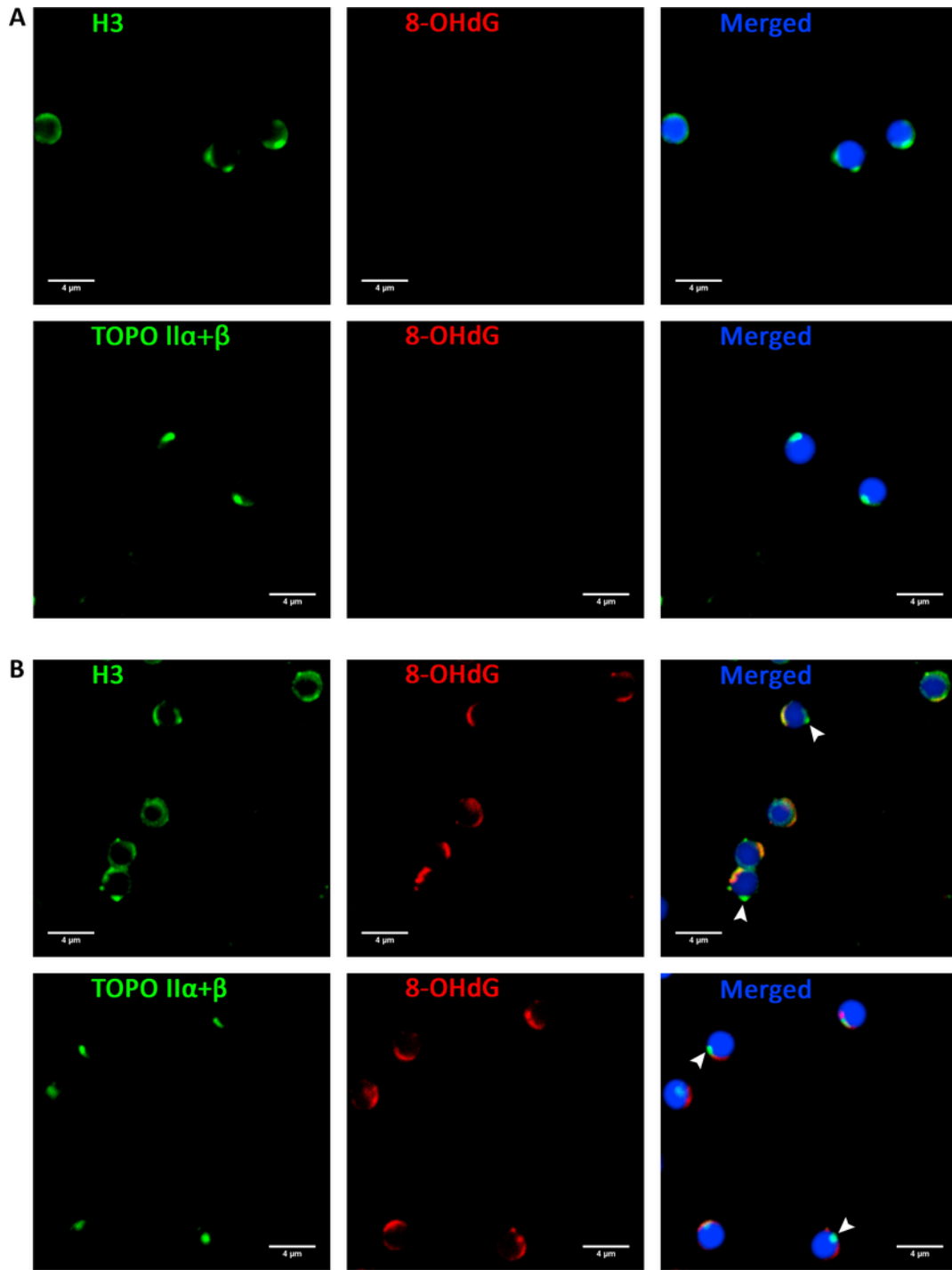
Fig. 4. Location of oxidative damage, histone H3 and nuclear matrix protein TOPO IIα+β after oxidative stress in sperm. Double immunolabelling of 8-OHdG with histone H3 or TOPO IIα+β were carried out on untreated (A) or H_2O_2-treated sperm spreads (B). Representative confocal images show the oxidative DNA adduct in red, labelled with AlexaFluor®568, and the distribution of histone H3 or TOPO IIα+β in green, labelled with AlexaFluor®488. Arrow heads indicate those regions harboring the labelled protein which are not affected by oxidation. Merged images were overlapped using ZEN Blue software. Scale bar, 4 μm.

The study of the distribution of the oxidative lesions by 8-OHdG immunolabelling, the most predominant oxidative adduct, commonly used as a hallmark of oxidative DNA damage [29,30], also supports the previous observation. UV irradiation promoted the localization of 8-OHdG in whole nucleus of zebrafish spermatozoa due to its ability to penetrate and directly affect the whole genome despite the presence of different chromatin blocks or nuclear proteins. Distribution of 8-OHdG revealed a specific pattern after H_2O_2 treatment, remaining peripheral around the sperm nucleus, which suggests greater exposure of genes located in these regions to ROS. This is in agreement with previous results in trout spermatozoa [11] and reinforces the idea of differential accessibility of harmful agents to sperm chromatin. Images show the location of histone H3, an indicator of more relaxed nucleosomal regions, mainly peripheral. The distribution is

very similar to that observed for 8-OHdG after H_2O_2 treatment, but not after other genotoxic injuries. TOPO IIα+β, a nuclear matrix protein absent from the most compacted regions, appears as a clear and peripheral spot that does not perfectly match with the oxidative lesions promoted by H_2O_2. Peroxiporins, which are responsible for guiding the efflux of H_2O_2 into the cell [31] and potentially to the nuclear periphery, have been described as spermatozoa-specific aquaporins. Therefore, susceptibility observed after oxidative stress may be determined by the accessibility of ROS to the different nuclear territories rather than by chromatin packaging or epigenetic marks. Freezing/thawing promoted the localization of 8-OHdG over the entire nucleus in some cells, which is different from the situation observed in rainbow trout sperm [11].

5. Conclusions

The location of nucleosomes or nuclear matrix proteins in sperm chromatin, in the most accessible regions to the transcription machinery, does not render specific genes and chromatin areas more vulnerable to damage in zebrafish. Susceptibility was related to the type of injuring agent. Access by the damaging agent to the sperm nucleus could be the greatest determinant in the distribution of sperm DNA damage in zebrafish. Our results demonstrate that the genes evaluated in this study are not particularly sensitive to a range of DNA injuring agents, and consequently these genes or their integrity, cannot be used as sentinels or biomarkers of genetic damage.

Conflicts of interest

The authors declare that no conflict of interest exists.

Acknowledgements

References

[1] D. Evenson, L. Jost, Sperm chromatin structure assay is useful for fertility assessment, Meth Cell Sci 22 (2000) 169–189.

[2] B.E. Speyer, A.R. Pizzey, M. Ranieri, R. Joshi, J.D.A. Delhanty, P. Serhal, Fall in implantation rates following ICSI with sperm with high DNA fragmentation, Hum Reprod 25 (2010) 1609–1618, https://doi.org/10.1093/humrep/deq116.

[3] W.S. Ward, Function of sperm chromatin structural elements in fertilization and development, Mol Hum Reprod 16 (2010) 30–36, https://doi.org/10.1093/molehr/gap080.

[4] U. Brykczynska, M. Hisano, S. Erkek, L. Ramos, E.J. Oakeley, T.C. Roloff, et al., Repressive and active histone methylation mark distinct promoters in human and mouse spermatozoa, Nat Struct Mol Biol 17 (2010) 679–687, https://doi.org/10.1038/nsmb.1821.

[5] Y. Yamauchi, J.A. Shaman, W.S. Ward, Non-genetic contributions of the sperm nucleus to embryonic development, Asian J Androl 13 (2011) 31–35, https://doi.org/10.1038/aja.2010.75.

[6] S.S. Hammoud, D.A. Nix, H. Zhang, J. Purwar, D.T. Carrell, B.R. Cairns, Distinctive chromatin in human sperm packages genes for embryo development, Nature 460 (2009) 473–478, https://doi.org/10.1038/nature08162.

[7] D. Miller, M. Brinkworth, D. Iles, Paternal DNA packaging in spermatozoa: more than the sum of its parts? DNA, histones, protamines and epigenetics, Reproduction 139 (2010) 287–301, https://doi.org/10.1530/REP-09-0281.

[8] A. Champroux, J. Torres-Carreira, P. Gharagozloo, J.R. Drevet, A. Kocer, Mammalian sperm nuclear organization: resiliencies and vulnerabilities, Basic Clin Androl 26 (2016) 17, https://doi.org/10.1186/s12610-016-0044-5.

[9] A. Noblanc, C. Damon-Soubeyrand, B. Karrich, J. Henry-Berger, R. Cadet, F. Saez, et al., DNA oxidative damage in mammalian spermatozoa: where and why is the male nucleus affected?, Free Radic Biol Med 65 (2013) 719–723, https://doi.org/10.1016/j.freeradbiomed.2013.07.044.

[10] L.J. Frehlick, J.M. Eirín-lópez, A. Prado, Su HW. Harvey, H.E. Kasinsky, J. Ausió, Sperm nuclear basic proteins of two closely related species of scorpaeniform fish (Sebastes maliger, Sebastolobus sp.) with different sexual reproduction and the evolution of fish protamines, J Exp Zool Part A Comp Exp Biol 305A (2006) 277–287, https://doi.org/10.1002/jez.a.239.

[11] S. González-Rojo, C. Fernández-Díez, S.M. Guerra, V. Robles, M.P. Herráez, Differential gene susceptibility to sperm DNA damage: analysis of developmental key genes in trout, PLoS One 9 (2014)e114161https://doi.org/10.1371/journal.pone.0114161.

[12] S.-F. Wu, H. Zhang, B.R. Cairns, Genes for embryo development are packaged in blocks of multivalent chromatin in zebrafish sperm, Genome Res 21 (2011) 578–589, https://doi.org/10.1101/gr.113167.110.

[13] C. Carmichael, M. Westerfield, Z.M. Varga, Cryopreservation and in vitro fertilization at the zebrafish international resource center, Meth Mol Biol 546 (2009) 45–65, https://doi.org/10.1007/978-1-60327-977-2_4.

[14] Rothfuss O, Gasser T, Patenge N. Analysis of differential DNA damage in the mitochondrial genome employing a semi-long run real-time PCR approach. Nucleic Acids Res 2010;38:e24–e24. doi:10.1093/nar/gkp1082.

[15] S. Kawanishi, Y. Hiraku, S. Oikawa, Mechanism of guanine-specific DNA damage by oxidative stress and its role in carcinogenesis and aging, Mutat Res 488 (2001) 65–76.

[16] B. Epe, DNA damage spectra induced by photosensitization, Photochem Photobiol Sci 11 (2012) 98–106, https://doi.org/10.1039/c1pp05190c.

[17] G.J. Dietrich, A. Szpyrka, M. Wojtczak, S. Dobosz, K. Goryczko, Ł. Żakowski, et al., Effects of UV irradiation and hydrogen peroxide on DNA fragmentation, motility and fertilizing ability of rainbow trout (Oncorhynchus mykiss) spermatozoa, Theriogenology 64 (2005) 1809–1822, https://doi.org/10.1016/j.theriogenology.2005.04.010.

[18] N. Saperas, M. Chiva, D.C. Pfeiffer, H.E. Kasinsky, J. Ausió, Sperm nuclear basic proteins (SNBPs) of agnathans and chondrichthyans: variability and evolution of sperm proteins in fish, J Mol Evol 44 (1997) 422–431.

[19] F. Cartón-García, M.F. Riesco, E. Cabrita, M.P. Herráez, V. Robles, Quantification of lesions in nuclear and mitochondrial genes of Sparus aurata cryopreserved sperm, Aquaculture 402–403 (2013) 106–112, https://doi.org/10.1016/J.AQUACULTURE.2013.03.034.

[20] L.K. Thomson, S.D. Fleming, R.J. Aitken, G.N. De Iuliis, J.-A. Zieschang, A.M. Clark, Cryopreservation-induced human sperm DNA damage is predominantly mediated by oxidative stress rather than apoptosis, Hum Reprod 24 (2009) 2061–2070, https://doi.org/10.1093/humrep/dep214.

[21] N. Zribi, N.F. Chakroun, F. Ben Abdallah, H. Elleuch, A. Sellami, J. Gargouri, et al., Effect of freezing–thawing process and quercetin on human sperm survival and DNA integrity, Cryobiology 65 (2012) 326–331, https://doi.org/10.1016/j.cryobiol.2012.09.003.

[22] S. Pérez-Cerezales, S. Martínez-Páramo, E. Cabrita, F. Martínez-Pastor, P. de Paz, M.P. Herráez, Evaluation of oxidative DNA damage promoted by storage in sperm from sex-reversed rainbow trout, Theriogenology 71 (2009) 605–613, https://doi.org/10.1016/j.theriogenology.2008.09.057.

[23] N. Zribi, N. Feki Chakroun, H. El Euch, J. Gargouri, A. Bahloul, L. Ammar Keskes, Effects of cryopreservation on human sperm deoxyribonucleic acid integrity, Fertil Steril 93 (2010) 159–166, https://doi.org/10.1016/j.fertnstert.2008.09.038.

[24] C. Tatone, G. Di Emidio, M. Vento, R. Ciriminna, P.G. Artini, Cryopreservation and oxidative stress in reproductive cells, Gynecol Endocrinol 26 (2010) 563–567, https://doi.org/10.3109/09513591003686395.

[25] S. Pérez-Cerezales, A. Gutiérrez-Adán, S. Martínez-Páramo, J. Beirão, M.P. Herráez, Altered gene transcription and telomere length in trout embryo and larvae obtained with DNA cryodamaged sperm, Theriogenology 76 (2011) 1234–1245, https://doi.org/10.1016/j.theriogenology.2011.05.028.

[26] E. Cabrita, V. Robles, L. Rebordinos, C. Sarasquete, M.P. Herráez, Evaluation of DNA damage in rainbow trout (Oncorhynchus mykiss) and gilthead sea bream (Sparus aurata) cryopreserved sperm, Cryobiology 50 (2005) 144–153, https://doi.org/10.1016/j.cryobiol.2004.12.003.

[27] S. Martínez-Páramo, P. Diogo, M.T. Dinis, F. Soares, C. Sarasquete, E. Cabrita, Effect of two sulfur-containing amino acids, taurine and hypotaurine in European sea bass (Dicentrarchus labrax) sperm cryopreservation, Cryobiology 66 (2013) 333–338, https://doi.org/10.1016/j.cryobiol.2013.04.001.

[28] E. Figueroa, I. Valdebenito, O. Merino, A. Ubilla, J. Risopatrón, J.G. Farias, Cryopreservation of Atlantic salmon Salmo salar sperm: effects on sperm physiology, J Fish Biol 89 (2016) 1537–1550, https://doi.org/10.1111/jfb.13052.

[29] G.M. Benhusein, E. Mutch, S. Aburawi, F.M. Williams, Genotoxic effect induced by hydrogen peroxide in human hepatoma cells using comet assay, Libyan J Med (2010) 5, https://doi.org/10.3402/ljm.v5i0.4637.

[30] G.P. Bienert, F. Chaumont, Aquaporin-facilitated transmembrane diffusion of hydrogen peroxide, Biochim Biophys Acta 1840 (2014) 1596–1604, https://doi.org/10.1016/j.bbagen.2013.09.017.

[31] H. Sies, Role of metabolic H_2O_2 generation: redox signaling and oxidative stress, J Biol Chem 289 (2014) 8735–8741, https://doi.org/10.1074/jbc.R113.544635.